

Synthesis of Calcium Carbonate Hollow Microspheres and the Pelletization Mechanism by Electrostatic Attraction of PEG–SDS

Lei Wang,* Zeen Yv, Licheng Ma, Qi Zheng, Tong Wang,* Xiaokui Che,* Xinglan Cui, Hongxia Li, Shenyu Wei, and Xinyue Shi



Cite This: *ACS Omega* 2023, 8, 42225–42234



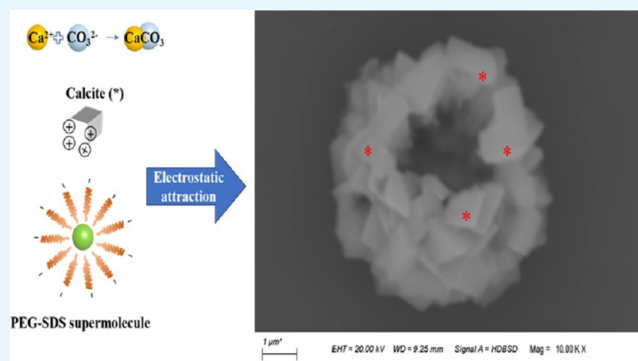
Read Online

ACCESS |

Metrics & More

Article Recommendations

ABSTRACT: Calcium carbonate is a common natural mineral with a wide range of applications. In this study, hollow calcite microspheres were successfully synthesized by using calcium chloride and sodium carbonate as raw materials in an SDS–PEG system. The results suggested that the appropriate concentration of SDS is necessary during the spherical crystallization of calcium carbonate. It was found that the crystals started to aggregate under the effect of SDS, and aggregation was enhanced with an increase in SDS concentration, leading to the transformation from hollow to solid microspheres. However, high temperatures will lead to the transformation from calcite to aragonite, resulting in the collapse of the formed spherical structure. Infrared spectroscopy and conductivity analysis suggested that when the concentration of SDS reached 0.3 g/L in the PEG–SDS system, SDS and PEG formed a spherical supramolecular structure. This structure could act as a template, leading to the aggregation of calcite through electrostatic attraction and finally to the formation of a hollow spherical structure.



1. INTRODUCTION

Calcium carbonate is a common mineral in nature that is widely used in industry. However, natural calcium carbonate needs to be regulated to meet the needs of different conditions due to its different polymorphs and morphologies. Generally, calcium carbonate has three different polymorphs, vaterite, aragonite, and calcite, whose thermodynamic stability increases in this order.^{1–3} Several studies have been conducted on the morphology and polymorphic control of calcium carbonate.^{4–8} Among them, spherical calcium carbonate has been widely studied because of its simple structure, good smoothness, and fluidity.^{9–13} Studies have shown that adding additives is one of the most effective methods for the morphology control of calcium carbonate. Zheng et al.¹⁴ successfully prepared spherical calcium carbonate with poly(acrylic acid) and sodium dodecyl benzenesulfonate, which indicated that the morphology of calcium carbonate can be controlled by anionic surfactants and anionic polymers. Ramesh et al.¹⁵ found that in the water–methanol system, the polymorph of calcium carbonate can be controlled by adjusting the pH. When pH < 8, vaterite and calcite could crystallize simultaneously, while only vaterite could crystallize from the solution when pH > 8. Xia et al.¹⁶ used PSS as an additive to prepare spherical and olive-shaped vaterite by mixed deposition in aqueous solution and dimethyl sulfoxide (DMSO)–aqueous solution, respectively. However, most of the

research still focuses on the control of vaterite calcium carbonate microspheres. As the most thermodynamically unstable polymorph, vaterite will easily transform into stable calcite, resulting in the collapse of the spherical morphology.^{17–22} Therefore, it may be difficult for vaterite calcium carbonate microspheres to maintain their morphology, which would limit their further application. Compared with vaterite microspheres, calcite microspheres are more favored for their long-standing maintenance of the original shape. However, few studies have been conducted on the control of calcite microspheres.

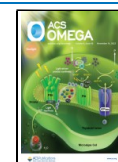
In this study, hollow calcite microspheres were successfully synthesized by using poly(ethylene glycol) (PEG)–sodium dodecyl sulfate (SDS) as additives. It was found that the concentration of additives and the temperature of the reaction system could significantly affect the morphology of calcite crystals, and PXRD, FTIR, and SEM were conducted to further investigate the morphology and polymorphic evolution of the crystals. In addition, the regulating mechanism of PEG–SDS

Received: June 12, 2023

Revised: September 21, 2023

Accepted: October 13, 2023

Published: October 31, 2023



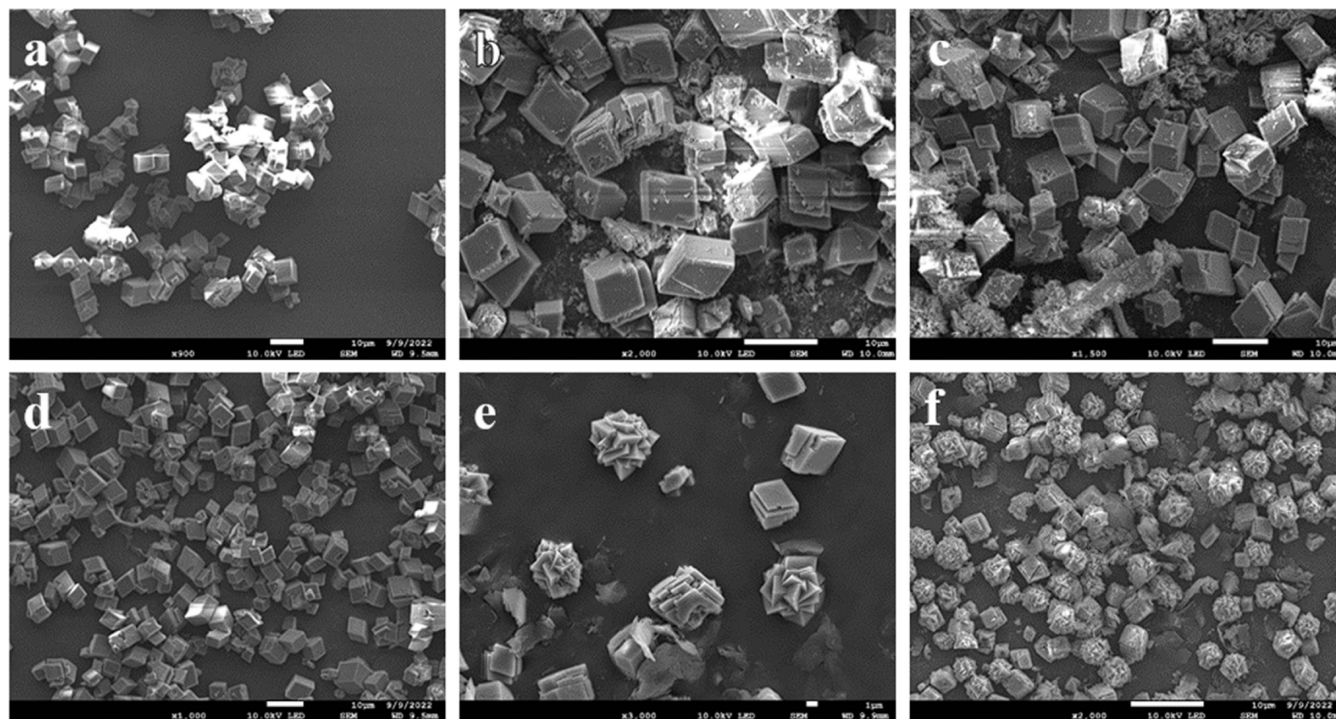


Figure 1. SEM images of the samples with different concentrations of additives: (a) PEG 10 g/L, (b) PEG 15 g/L, (c) PEG 25 g/L, (d) SDS 1 g/L, (e) SDS 3 g/L, and (f) SDS 4 g/L.

supramolecules was analyzed, and finally, the process of spherical crystallization of calcite was proposed.

2. MATERIALS AND METHODS

2.1. Materials. Sodium carbonate (Na_2CO_3), calcium chloride (CaCl_2), and sodium dodecyl sulfonate (SDS) were purchased from Xi Long Chemical Factory (Shantou, China), and poly(ethylene glycol) (PEG) (average Mn 400) was purchased from Aladdin Biochemical Technology Co. Ltd. (Shanghai, China). All chemicals were of analytical grade and used without further purification.

2.2. Preparation of Hollow Microspheres of CaCO_3 . An equal volume of 25 g/L PEG solution was added to 0.1 mol/L CaCl_2 solution and Na_2CO_3 solution, respectively, and the solution was placed in a water bath at different temperatures and stirred for 30 min. A certain amount of SDS was added to Na_2CO_3 solution and continued to be stirred for 30 min. Finally, the Na_2CO_3 solution was quickly introduced into CaCl_2 solution and continuously stirred for 2 h. Then, the solution was filtered and washed, and the solid was dried in the oven (80 °C) for 8 h to obtain hollow microspheres of CaCO_3 .

2.3. Characterization. Morphologies of the synthesized CaCO_3 microparticles were characterized by scanning electron microscopy (SEM, TM3000, Hitachi, Japan) with an accelerating voltage of 10 kV. The crystallographic structure of the microspheres was identified with a Rigaku MiniFlex-600 X-ray diffractometer (Rigaku, Japan) using $\text{Cu K}\alpha$ radiation ($\lambda = 1.54184 \text{ \AA}$) at 40 kV and 15 mA, in the 2θ range of 10–90° with a scan rate of 10.0°/min. All data were obtained at ambient temperature. FTIR spectra were collected with a Bruker α ATR platinum instrument in the wavenumber range of 4000–500 cm^{-1} , with a resolution of 4 cm^{-1} under ambient conditions.

3. RESULTS AND DISCUSSION

3.1. Growth of CaCO_3 Hollow Spheres in the Presence of SDS. First, the influence of single additives on the crystallization of calcium carbonate was studied. Figure 1 shows that when PEG alone was added to the solution, only cube-like crystals were obtained, regardless of its concentration (Figure 1a–c). The same observation was made when SDS was added to the solution with a concentration of 1 g/L (Figure 1d), but when the concentration of SDS increased, calcium carbonate started to crystallize into a multilayered flower morphology (Figure 1e,f). However, still, no spherical crystals formed in the solution with the addition of SDS.

Based on the above results, we continued to study whether there exists some synergistic effect of the two additives. Figure 2 shows the SEM images of the obtained samples with different concentrations of SDS in the presence of PEG (25 g/L). It could be found that when no SDS was added to the solution, typical cubic CaCO_3 crystallized from the solution. When the concentration of SDS is 1 g/L, spherical crystals appeared, with partially cubic CaCO_3 crystals. When the amount of SDS was increased to 3 g/L, all of the CaCO_3 crystals aggregated into hollow microspheres with a diameter of 8–10 μm . However, when the amount of SDS reached 4 g/L, hollow calcium carbonate gradually disappeared and solid calcium carbonate microspheres formed. This result reveals that the synergistic effect of the two additives may be responsible for the formation of the hollow spherical crystal.

To verify whether the polymorphic transition occurs during the spherical crystallization, PXRD was performed for different samples, whose results are illustrated in Figure 3. The PXRD patterns revealed that the polymorphic transition did not occur regardless of the concentration of SDS, and a comparison with the PDF card indicated that the samples existed in the calcite form. The characteristic reflection at 2θ values of 23.054, 29.4,

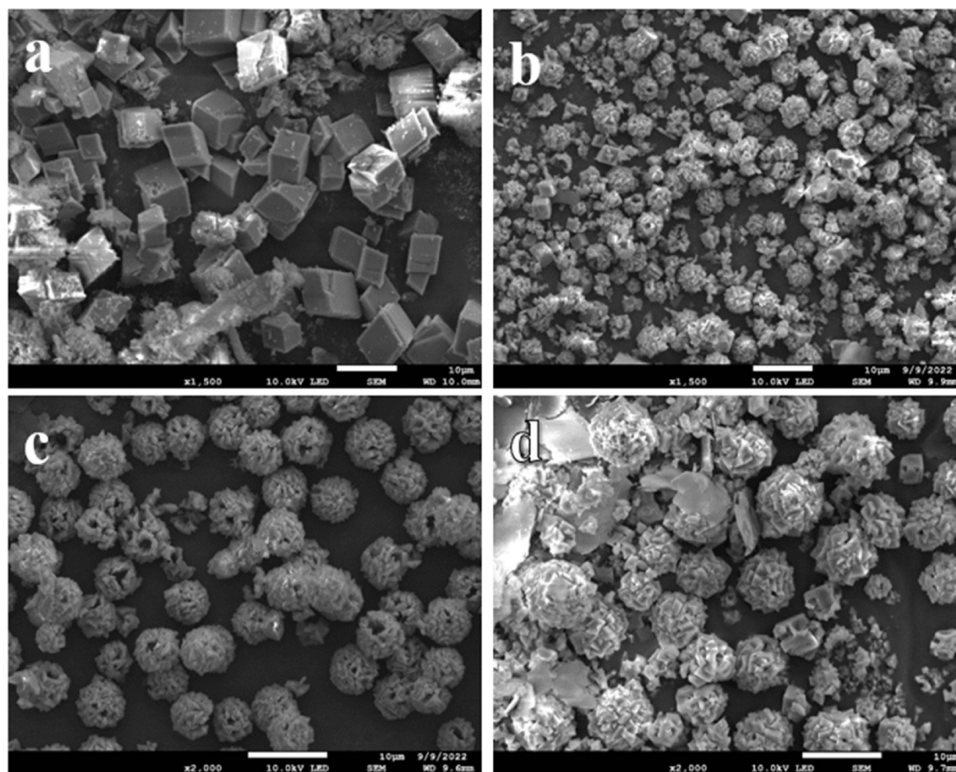


Figure 2. SEM images of the obtained samples with different SDS concentrations in the presence of PEG (25 g/L): (a) 0, (b) 1, (c) 3, and (d) 4 g/L SDS.

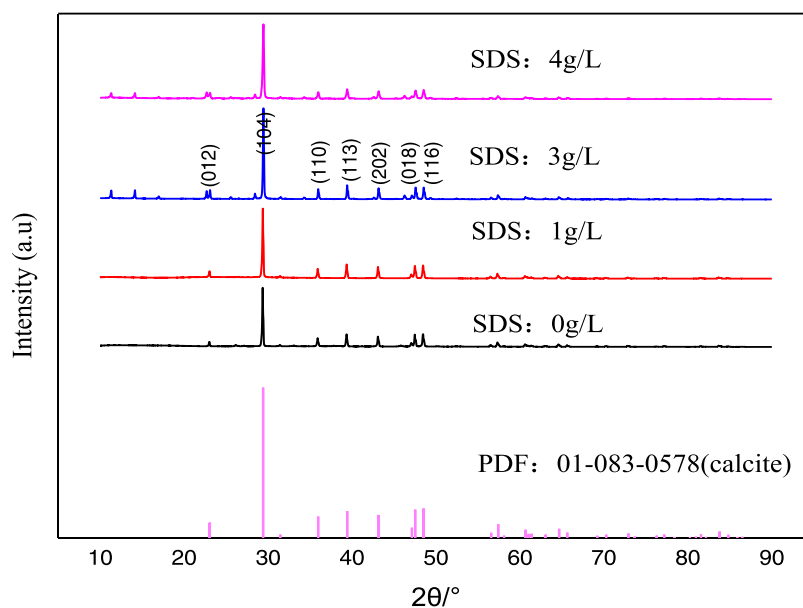


Figure 3. PXRD patterns of the samples obtained with different SDS concentrations (%).

35.969, 39.409, 43.158, 47.506, and 48.505° correspond to the hkl planes of (102), (104), (110), (113), (202), (018), and (116), respectively. The peak values of the PXRD spectrum were normalized, and the orientation uniformity during the formation of calcite under different conditions was quantitatively analyzed. The uniformity is determined by the following formula:²³

$$\%hkl = \frac{I_{(hkl)}/I_{hkl}^*}{\sum_{hkl} (I_{(hkl)}/I_{hkl}^*)} * 100\%$$

where $I(hkl)$ represents the actual peak intensity of the sample and $I^*(hkl)$ represents the diffraction peak intensity of the corresponding crystal plane of the standard intensity. The results are presented in Table 1.

As shown in Table 1, the orientation uniformity of calcite crystals precipitated in different solutions is basically the same, which indicates that the additives have limited effect on the polymorphic form of CaCO_3 . Nevertheless, only if SDS coexists with PEG in the solution, CaCO_3 tends to aggregate into spheres. This may imply that there is a synergistic effect between

Table 1. PXRD Data of the Crystallographic Orientation of Calcite Crystals Precipitated from Different Systems

<i>hkl</i>	standard intensity	SDS 0 g/L, PEG 0 g/L		SDS 0 g/L PEG 25 g/L		SDS 3 g/L PEG 25 g/L	
		$I_{(hkl)}$	% <i>hkl</i>	$I_{(hkl)}$	% <i>hkl</i>	$I_{(hkl)}$	% <i>hkl</i>
102	9.6	32802	17.60	10986	12.74	25223	17.88
104	100	309194	15.93	108323	12.06	239852	16.32
110	13.3	34775	13.47	16686	13.97	27800	14.22
113	18.5	50750	14.13	23833	14.34	37667	13.85
202	14.3	35624	12.84	17302	13.47	29929	14.24
018	18.0	46515	13.31	29743	18.39	31944	12.07
116	19.0	46865	12.71	25652	15.03	31896	11.42

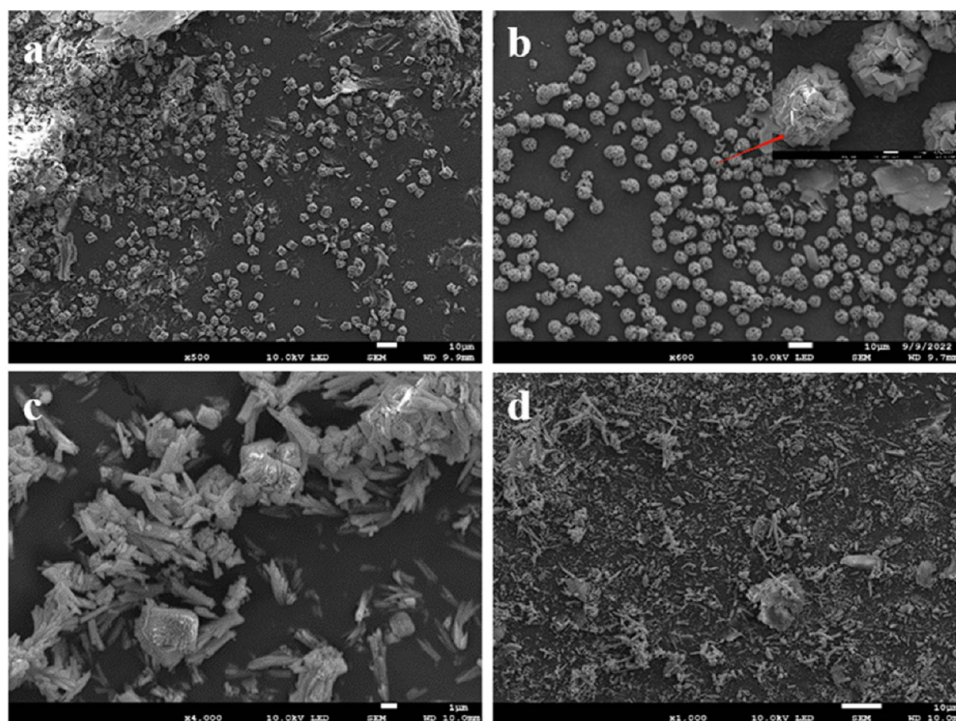


Figure 4. SEM images of the obtained samples at different temperatures: (a) 20, (b) 40, (c) 60, and (d) 80 °C.

the polymer and the surfactant on the formation of spherical calcium carbonate.

3.2. Influence of Temperature. The temperature also has a significant influence on the morphology of CaCO_3 , especially in the presence of the polymer and surfactant. Temperature may affect the interactions between the polymer and surfactant, thus further affecting the growth and aggregation of calcium carbonate. The morphology of the precipitated CaCO_3 under different temperatures is shown in Figure 4, with the concentration of SDS at 3 g/L.

Figure 4a shows that at a relatively lower temperature (20 °C), the synthesized calcium carbonate precipitates are mainly cubic crystals without spherical aggregation, which is supposed to be calcite, the most thermally stable polymorph. Nevertheless, when the temperature was increased to 40 °C, the crystals began to agglomerate into hollow spheres (Figure 4b), indicating the variation in the interactions between the particles in the solution. However, at this time, it is obvious that the spherical particles are still composed of cubic crystals. As the temperature increased continuously (60 and 80 °C, Figure 4c,d), the original spherical aggregates collapsed, while rodlike crystals formed, suggesting that the state of the solution changed again with the temperature varying.

To verify whether polymorphic transition occurred with an increase in temperature, PXRD was conducted for the samples, as shown in Figure 5. The PXRD analysis suggests that when the temperature is 20–40 °C, the PXRD diffraction characteristic peak of the sample corresponds to PDF 01–083–0453, indicating that the crystals are mainly calcite, which is consistent with the SEM morphology analysis. However, when the temperature reached 60 °C, the morphology of the crystals changed and a large number of short rods appeared. PXRD analysis shows that the diffraction characteristic peak is consistent with PDF 00–005–0453, indicating that calcite calcium carbonate gradually converts to aragonite. These results indicate that temperature may affect the interactions between the SDS, PEG, and the calcite crystal surfaces, resulting in both morphology and polymorph transition.

3.3. Influence of Reaction Time. To explore the formation process of the calcium carbonate microsphere, the morphology of calcium carbonate under different reaction time conditions was analyzed, and the results are shown in Figure 6. It can be seen from the SEM that after reaction for 0.5h, calcium carbonate microspheres were generated in the solution, and with the crystallization reaction proceeding, more microspherical crystals formed in the solution, and nearly all of the calcium carbonate crystals aggregated into larger spherical crystals after

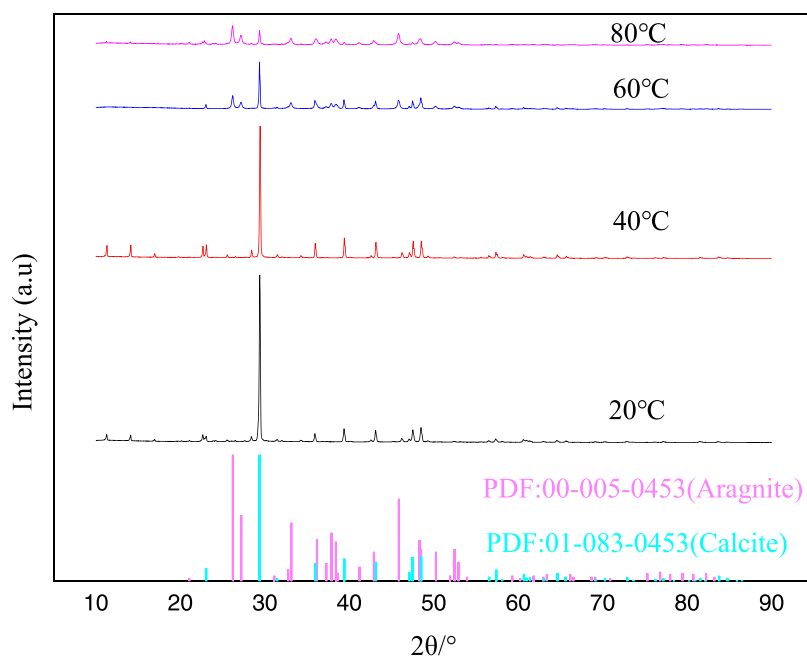


Figure 5. PXRD patterns of the samples obtained at different temperatures.

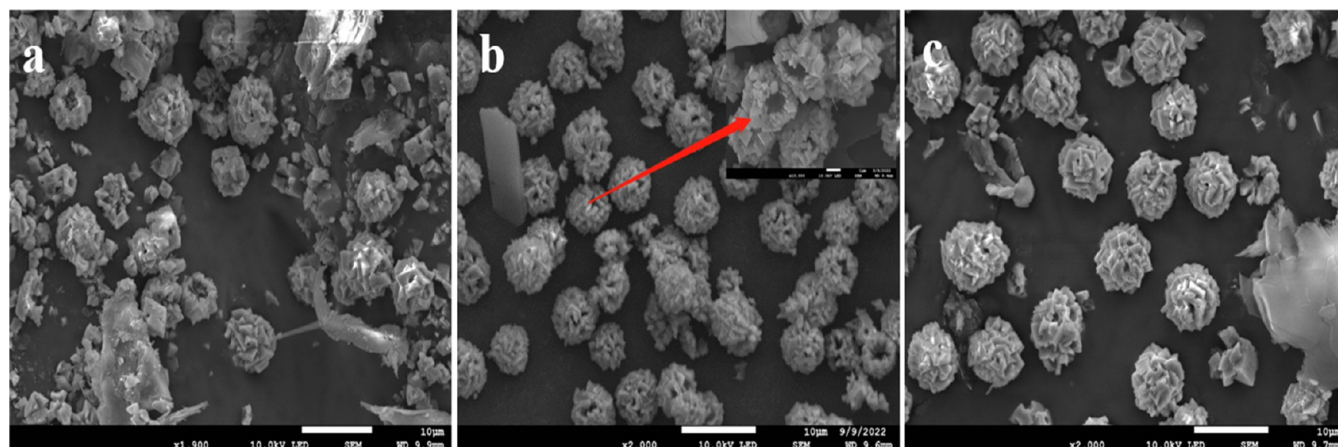


Figure 6. SEM image of the product with different reaction times: (a) 0.5, (b) 2, and (c) 3 h.

2h. At this time, holes could be found on the surface of the spherical crystals, suggesting their hollow structures. However, at 3 h, the holes became smaller and finally disappeared, resulting in a spherical crystal with an intact surface. By comparing the PXRD spectra with PDF cards (Figure 7), it could be suggested that the samples are calcite and that no polymorph transition occurred during the whole process.

3.4. Growth Mechanism for the Formation of Hollow CaCO_3 Microspheres. In order to understand the composition of the product, SEM and EDS surface scanning analyses were conducted. As the unique elements in calcium carbonate and SDS, the presence of Ca and S can be used to distinguish the presence of calcium carbonate and SDS. As shown in Figure 8, the distribution of Ca is consistent with that of microspheres in the SEM image, indicating that the products are mainly CaCO_3 . The EDS of S suggested that SDS (Figure 8c) also exists in the product, although in small amounts, and further overlay of the mapping supposed that some of the SDS was distributed on the surface of microspheres (Figure 8d). This indicated that the additives exhibit some interactions with the crystal faces, which

may play a dominant role in the formation of spherical calcium carbonate.

To better understand the formation of spherical calcite, FTIR spectroscopy was performed, and the results are illustrated in Figure 9. It could be found that all of the samples showed absorption peaks at around 1385 , 872 , and 712 cm^{-1} , which corresponded to standard calcite,^{24–26} indicating that the structure of the synthesized spherical calcium carbonate was that of calcite. However, in PEG–SDS and PEG systems, a chemical shift occurs in these peaks, which may be attributed to the addition of SDS and PEG. In addition, compared with pure calcium carbonate, calcium carbonate synthesized in the PEG–SDS system showed new absorption peaks at 2912 , 2844 , 1175 , and 1055 cm^{-1} ,^{27,28} which corresponded to the vibration of the C–H and alkyl sulfur groups of SDS molecules, respectively. Because of the fact that the samples were washed with deionized water after filtration, it could be supposed that SDS participated in the formation of spherical calcium carbonate and was left inside the spheres, again indicating that SDS may serve as a template to induce the formation of spherical calcite.

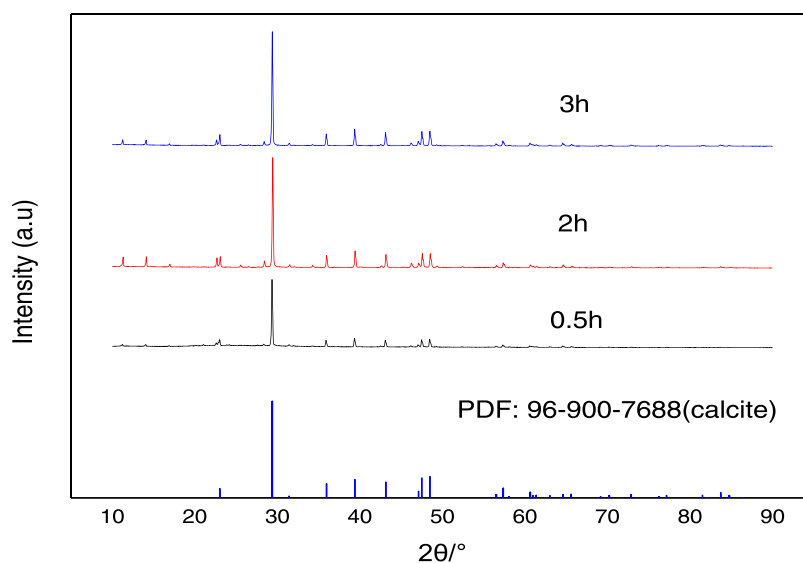


Figure 7. PXRD patterns of the sample.

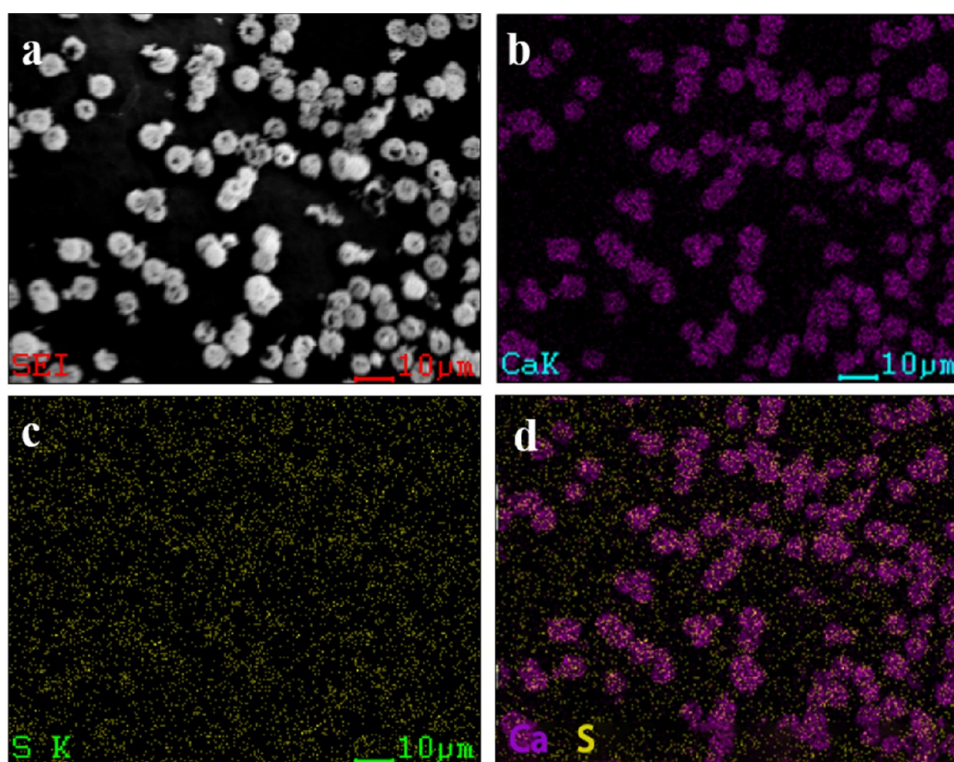


Figure 8. (a) SEM image and (b–d) EDS of the product.

To further determine the role of additives in the formation of spherical crystals, the conductivity of the solution (temperature: 40 °C; PEG 25 g/L; different concentrations of SDS) was tested to characterize the state of SDS molecules with different concentrations in the PEG–water system. As shown in Figure 10, it was found that the conductivity of the solution increased gradually with an increase in the SDS concentration. The slope of different points represents different states of the solution. When the SDS concentration reached 3 g/L (point A), the conductivity of the solution showed an obvious decrease, which indicates the formation of clusters. When the SDS concentration reached 4 g/L (point B), the conductivity of the solution showed an obviously increasing trend, indicating that the properties of

the solution changed again, and it can be seen obviously that a white floc appears in the solution, which means that the state of the original solution has been broken. Meanwhile, the surface of calcite crystals was also analyzed in detail to confirm the electrostatic force between calcite and the SDS–PEG polymer. According to the zeta potential of the calcite shown in Figure 11, when the solution is neutral, the surface of calcite is positive. This means that the calcite crystals could probably be induced by the SDS–PEG structure, which may be the main driving force for the formation of spherical crystals.

According to previous studies, it is believed that electrostatic forces or crystal growth are responsible for the formation of hollow spheres.^{29,30} Because of the electrostatic attraction, a

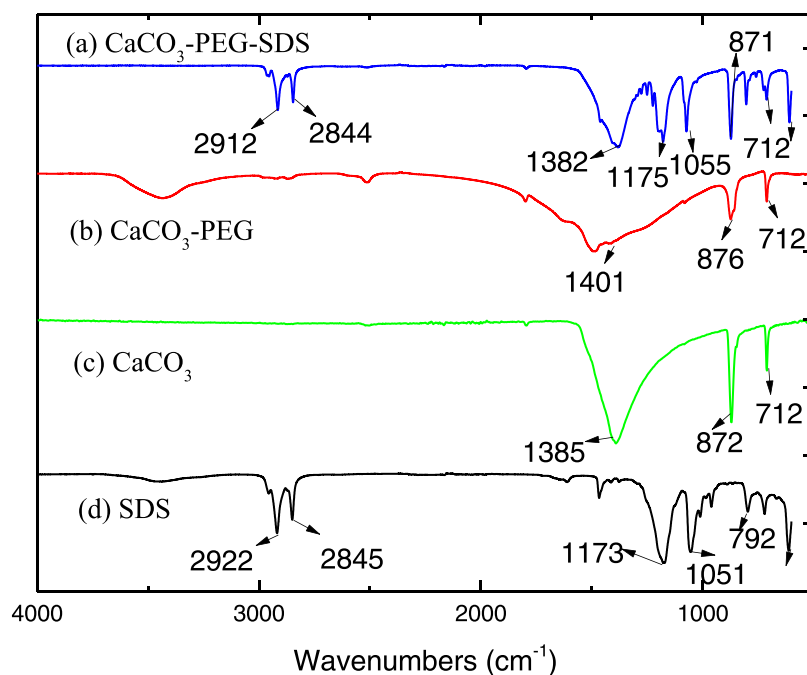


Figure 9. FTIR spectra of (a) CaCO_3 -PEG-SDS, (b) CaCO_3 -PEG, (c) CaCO_3 calcite, and (d) SDS at 40 °C.

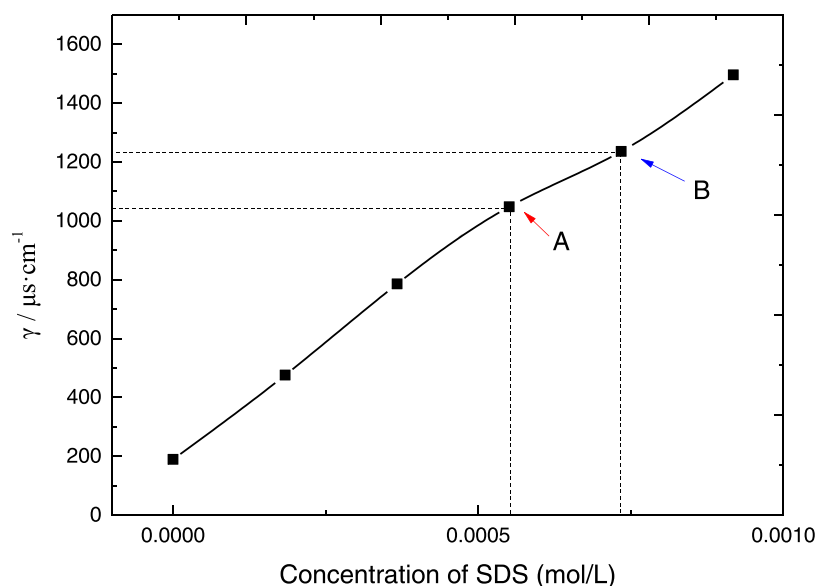


Figure 10. Variation of the conductivity with SDS concentration in the presence of 25 g/L PEG at 40 °C.

large amount of calcium ions would attach to the surface of the polymer first, followed by the attachment of CO_2 to the Ca^{2+} aggregates. Then, the initial calcium carbonate particles are formed, which eventually grow into spherical particles.^{31–33} However, in our study, the formation process of spherical CaCO_3 crystals is significantly different. According to the experiments above, the hollow spherical microspheres only formed when two additives were added in a specific proportion. Therefore, we speculate that there may be some interactions between SDS and PEG in the solution, resulting in the formation of SDS-PEG clusters, which could act as a template to induce the formation of spherical calcium carbonate. Based on the conclusion suggested above, a possible mechanism for the formation of a spherical crystal is proposed (Figure 12). First, the polymer and surfactant particles could interact in the

solution, resulting in the formation of free micelles and premicelles adsorbed on the polymers. When the concentration of SDS is sufficient, it could form a spherical structure with PEG in the solution, with its negative part exposed outside of the sphere. However, it has been verified that the surface of calcite crystals is usually positive, so the cubic calcite crystals approach the SDS-PEG structure and finally aggregate into hollow spheres. As the crystals continue growing, the hollows disappear and spheres become solid. However, at relatively higher temperatures, the calcite could transform into aragonite, along with a variation in the morphology, leading to the collapse of the spherical aggregates of crystals.

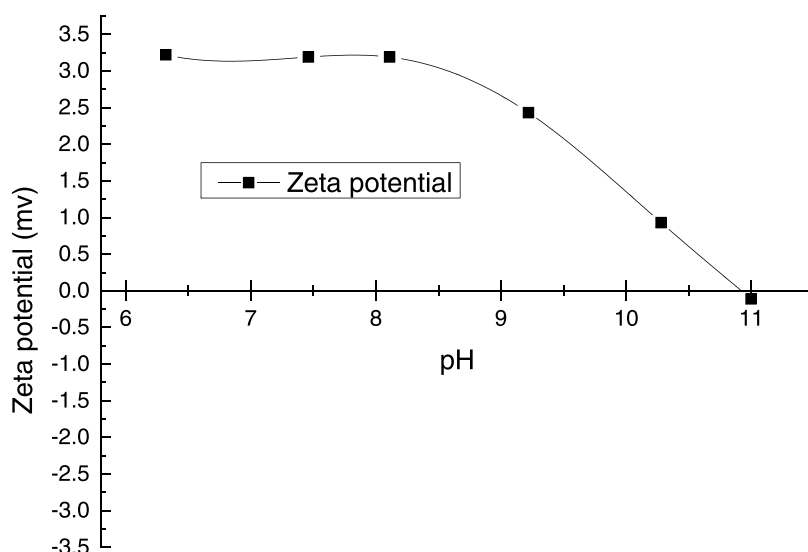


Figure 11. Relationship between the ζ potential of calcite and pH.

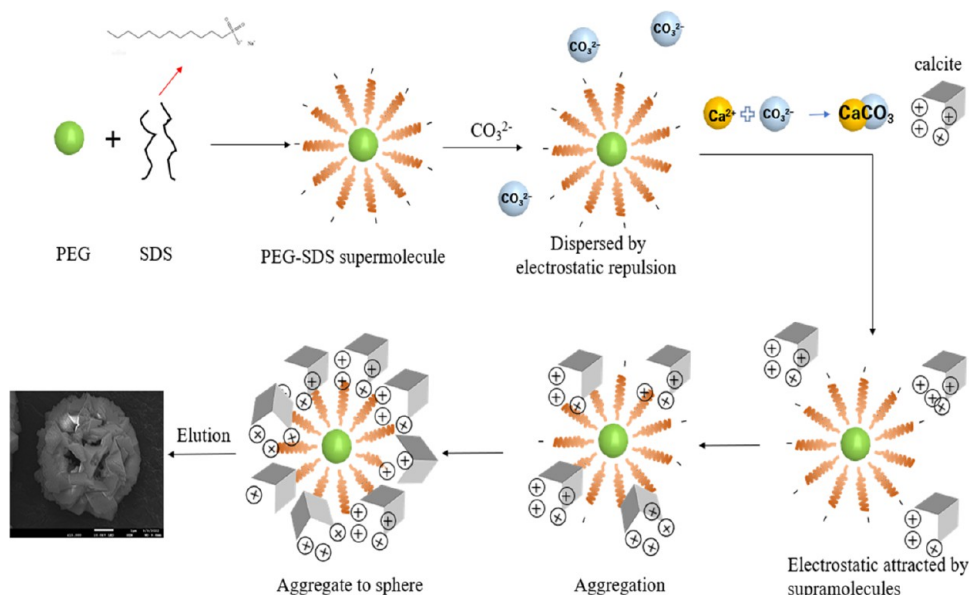


Figure 12. Schematic model of the formation mechanism of spherical CaCO_3 .

4. CONCLUSIONS

In summary, calcite CaCO_3 microspheres were successfully synthesized in the PEG–SDS system, and the morphology, aggregation state, and polymorphic form of calcium carbonate at different temperatures and SDS concentrations were described. The results showed that PEG and SDS could interact to form a spherical structure with negative surfaces, which could serve as a template in the aggregation process of calcium carbonate. Meanwhile, the surface of calcite crystals was verified as positive in a neutral solution, so the calcite crystals were attracted by the negatively charged PEG–SDS structures and aggregated into calcite hollow microspheres.

Compared with the vaterite reported in the previous literature, the spherical calcium carbonate we prepared in this study has a relatively larger crystal size (8–10 vs 0.05–5 μm) as well as better stability (at least 30 days vs 25 h at most; Table 2).^{34,35} Therefore, the spherical calcium carbonate we prepared in this study may have more advantages in applications such as

Table 2. Comparison of the Vaterite-Type and Calcite-Type Calcium Carbonate

property	vaterite-type calcium carbonate	calcite-type calcium carbonate
stability	≤ 25 h	≥ 30 days
size distribution	0.05–5 μm	8–10 μm
polymorph	vaterite	calcite
morphology	hollow microspheres	hollow microspheres

drug carriers, in the paper industry, or as adsorbents in the water treatment industry, which always requires long-term storage of the products.

AUTHOR INFORMATION

Corresponding Authors

Lei Wang – GRINM Resources and Environment Tech. Co., Ltd., Beijing 100088, China; Email: wanglei@grinm.com

Tong Wang – Beijing BECC Energy & Environment Engineering Technology Co., Ltd., Beijing 100040, China; Email: wangtong@becc.com.cn
Xiaokui Che – GRINM Resources and Environment Tech. Co., Ltd., Beijing 100088, China; Email: Xkche@grinm.com

Authors

Zeen Yv – GRINM Resources and Environment Tech. Co., Ltd., Beijing 100088, China
Licheng Ma – State Key Laboratory of Multiphase Complex Systems, Institute of Process Engineering, Chinese Academy of Sciences, Beijing 100190, China
Qi Zheng – GRINM Resources and Environment Tech. Co., Ltd., Beijing 100088, China
Xinglan Cui – GRINM Resources and Environment Tech. Co., Ltd., Beijing 100088, China
Hongxia Li – GRINM Resources and Environment Tech. Co., Ltd., Beijing 100088, China
Shenyv Wei – GRINM Resources and Environment Tech. Co., Ltd., Beijing 100088, China
Xinyue Shi – GRINM Resources and Environment Tech. Co., Ltd., Beijing 100088, China

Complete contact information is available at:

<https://pubs.acs.org/10.1021/acsomega.3c04068>

Author Contributions

Conceptualization and methodology: L.W.; validation and formal analysis: H.L.; investigation: Z.Y.; resources: L.M.; writing—original draft preparation: L.W.; writing—review and editing: T.W.; visualization: S.W. & X.S.; supervision: Q.Z., X.C., and X.C.; all authors have read and agreed to the published version of the manuscript.

Notes

The authors declare no competing financial interest.

ACKNOWLEDGMENTS

The authors are very thankful for the financial support from the National Key R&D Program of China (Project 2021YFC2900900).

REFERENCES

- (1) Mantilaka, M. M. M. G. P. G.; Pitawala, H. M. T. G. A.; Rajapakse, R. M. G.; et al. Formation of hollow bone-like morphology of calcium carbonate on surfactant/polymer templates. *J. Cryst. Growth* **2014**, *392*, 52–59.
- (2) Zhao, H.; Li, Y.; Liu, R.; Zhao, F.; Hu, Y. Synthesis method for silica needle-shaped nano-hollow structure. *Mater. Lett.* **2008**, *62*, 3401–3403.
- (3) Zhao, Z.; Zhang, L.; Da, H.; et al. Surfactant-assisted solvo- or hydrothermal fabrication and characterization of high-surface-area porous calcium carbonate with multiple morphologies. *Microporous Mesoporous Mater.* **2011**, *138* (1–3), 191–199, DOI: 10.1016/j.micromeso.2010.09.006.
- (4) Zhong, Q.; Li, W.; Su, X.; Li, G.; Zhou, Y.; Kundu, S. C.; Yao, J.; Cai, Y. Degradation pattern of porous CaCO₃ and hydroxyapatite microspheres in vitro and in vivo for potential application in bone tissue engineering. *Colloids Surf., B*, *143* 2016 56–63 DOI: 10.1016/j.colsurfb.2016.03.020.
- (5) Elbaz, N. M.; Owen, A.; Rannard, S.; McDonald, T. O. Controlled synthesis of calcium carbonate nanoparticles and stimuli-responsive multi-layered nanocapsules for oral drug delivery. *Int. J. Pharm.* **2020**, *574*, No. 118866.
- (6) Lai, Y.; Chen, L.; Bao, W.; et al. Glycine-mediated, selective preparation of mono-disperse spherical vaterite calcium carbonate in various reaction systems. *Cryst. Growth Des.* **2015**, *15* (3), 1194–1200.

- (7) Ajikumar, P. K.; Wong, L. G.; Subramanyam, G.; et al. Synthesis and characterization of monodispersed spheres of amorphous calcium carbonate and calcite spherules. *Cryst. Growth Des.* **2005**, *5* (3), 1129–1134.

- (8) Boyjoo, Y.; Pareek, V. K.; Liu, J. Synthesis of micro and nano-sized calcium carbonate particles and their applications. *J. Mater. Chem. A* **2014**, *2*, 14270–14288.

- (9) Zhao, D.; Jiang, J.; Xu, J.; et al. Synthesis of template-free hollow vaterite CaCO₃ microspheres in the H₂O/EG system. *Mater. Lett.* **2013**, *104*, 28–30.

- (10) Ji, X.; Li, G.; Huang, X. The synthesis of hollow CaCO₃ microspheres in mixed solutions of surfactant and polymer. *Mater. Lett.* **2008**, *62*, 751–754, DOI: 10.1016/j.matlet.2007.06.063.

- (11) Zheng, T.; Yi, H.; Zhang, S.; et al. Preparation and formation mechanism of calcium carbonate hollow microspheres. *J. Cryst. Growth* **2020**, *549*, No. 125870.

- (12) Jin, T.; Tian, X.; Hong, H.; et al. Study on preparation and crystalline transformation of nano- and micro-CaCO₃ by supercritical carbon dioxide. *Powder Technol.* **2020**, *370*, 29–38.

- (13) Yang, C.; Zhang, J.; Li, W.; Shang, S.; Guo, C. Synthesis of aragonite CaCO₃ nano-crystals by reactive crystallization in a high shear mixer. *Cryst. Res. Technol.* **2017**, *52*, No. 1700002, DOI: 10.1002/crat.201700002.

- (14) Zheng, T.; Zhang, X.; Yi, H. Spherical vaterite microspheres of calcium carbonate synthesized with poly (acrylic acid) and sodium dodecyl benzene sulfonate. *J. Cryst. Growth* **2019**, *528*, No. 125275.

- (15) Ramesh, T. N.; Inchara, S. A.; Pallavi, K. Para-amino benzoic acid-mediated synthesis of vaterite phase of calcium carbonate. *J. Chem. Sci.* **2015**, *127*, 843–848.

- (16) Xia, H.-Y.; Zhang, Q.; Wang, G.; et al. Study on Facile Fabrication of Spherical and Olivary Vaterite. *J. Synth. Cryst.* **2015**, *44*, 1701–1706.

- (17) Tobler, D. J.; Rodriguez-Blanco, J. D.; S?Rensen, H. O.; et al. The effect of pH on amorphous calcium carbonate (ACC) structure and transformation. *Cryst. Growth Des.* **2016**, *16*, 4500–4508, DOI: 10.1021/acs.cgd.6b00630.

- (18) Sand, K. K.; Rodriguez-Blanco, D.; Makovicky, E.; et al. Crystallization of CaCO₃ in Water–Alcohol Mixtures: Spherulitic Growth, Polymorph Stabilization, and Morphology Change. *Cryst. Growth Des.* **2012**, *12* (2), 842–853.

- (19) Wei, H.; Shen, Q. Influence of polyvinylpyrrolidone on the precipitation of calcium carbonate and on the transformation of vaterite to calcite. *J. Cryst. Growth* **2003**, *250*, 516–524, DOI: 10.1016/S0022-0248(02)02484-3.

- (20) Han, Y. S.; Hadiko, G.; Fuji, M.; Takahashi, M. Crystallization and transformation of vaterite at controlled pH. *J. Cryst. Growth* **2006**, *289*, 269–274, DOI: 10.1016/j.jcrysgro.2005.11.011.

- (21) Sarkar, A.; Dutta, K.; Mahapatra, S. Polymorph control of calcium carbonate using Insoluble layered double hydroxide. *Cryst. Growth Des.* **2013**, *13*, 204–211, DOI: 10.1021/cg301368v.

- (22) Falini, G.; Fermani, S.; Vanzo, S.; Miletic, M.; Zaffino, G. Influence on the formation of aragonite or vaterite by otolith macromolecules. *Eur. J. Inorg. Chem.* **2005**, *2005*, 162–167, DOI: 10.1002/ejic.200400419.

- (23) Shen, Q.; Wei, H.; Wang, L. Crystallization and Aggregation Behaviors of Calcium Carbonate in the Presence of Poly(vinylpyrrolidone) and Sodium Dodecyl Sulfate. *J. Phys. Chem. B* **2005**, *109*, 18342–18347, DOI: 10.1021/jp052094a.

- (24) Gopi, S. P.; Subramanian, V. K. Polymorphism in CaCO₃ effect of temperature under the influence of EDTA (di sodium salt). *Desalination* **2012**, *297*, 38–47.

- (25) Chen, S.; Yu, S.; Jiang, J.; Li, F.; Liu, Y. Polymorph discrimination of CaCO₃ mineral in an ethanol/water solution: formation of complex vaterite superstructures and aragonite rods. *Chem. Mater.* **2006**, *18*, 115–122.

- (26) Jiang, J.; Liu, J.; Liu, C.; Zhang, G.; Gong, X.; Liu, J. Roles of oleic acid during micropore dispersing preparation of nano-calcium carbonate particles. *Appl. Surf. Sci.* **2011**, *257*, 7047–7053.

(27) Catauro, M.; Bollino, F.; Papale, F.; et al. Investigation of the sample preparation and curing treatment effects on mechanical properties and bioactivity of silica rich metakaolingeo polymer. *Mater. Sci. Eng.: C* **2014**, *36*, 20–24.

(28) Flach, C. R.; Mao, G.; Saad, P. Confocal Raman and IR spectroscopic studies of SDS permeation in skin and interaction with stratum corneum lipids. In *Journal of the American Academy of Dermatology* 2011 DOI: 10.1016/j.jaad.2010.09.146.

(29) Wang, X.; Wei, M.; Liu, K. Research Progress on Control and Preparation of Vaterite-Type Calcium Carbonate. *J. Chin. Ceram. Soc.* **2022**, *41* (08), 2860–2870 + 2878, DOI: 10.16552/j.cnki.issn1001-1625.2022.08.013.

(30) Jiang, J. X.; Wu, Y.; He, Y.; et al. Progress in Tuning of Metastable Vaterite Calcium Carbonate. *J. Inorg. Mater.* **2017**, *32* (07), 681–690, DOI: 10.15541/jim20160484.

(31) Wei, H.; Shen, O.; Zhao, Y.; et al. Effect of anionic surfactant-polymer complexes on the crystallization of calcium carbonate. *J. Cryst. Growth* **2004**, *264* (1–3), 424–429.

(32) Wang, Y. S.; Moo, Y. X.; Chen, C. P.; et al. Fast precipitation of uniform CaCO₃ nanospheres and their transformation to hollow hydroxyapatite nanospheres. *J. Colloid Interface Sci.* **2010**, *352*, 393–400.

(33) Zhou, W. C. Structure and Formation Mechanism of Spherulites. *J. Fudan Univ.* **2022**, *61* (06), 653–661 + 669.

(34) Zhang, X. L.; B, Y. Study on synthesis and stability of vaterite calcium carbonate. *Inorg. Chem. Ind.* **2018**, *50* (2), 46–49.

(35) Wang, X.; Wei, M.; Liu, K. Research progress on control and preparation of vaterite-type calcium carbonate. *Bull. Chin. Ceram. Soc.* **2022**, *41* (8), 2860–2870 + 2878, DOI: 10.16552/j.cnki.issn1001-1625.2022.08.013.